Modeling epidemiological disturbances in LANDIS-II

Francesco Tonini[a,*,1], Chris Jones[a], Brian R. Miranda[b], Richard C. Cobb[c], Brian R. Sturtevant[b], Ross K. Meentemeyer[a,d]

[a]Center for Geospatial Analytics, North Carolina State University, Raleigh, NC

[b]USDA Forest Service, Northern Research Station, Rhinelander, WI

[c]Natural Resources Management and Environmental Sciences Department, California State Polytechnic University, San Luis Obispo, CA

[d]Forestry and Environmental Resources, North Carolina State University, Raleigh, NC

[*]Corresponding author

E-mail: ftonini84@gmail.com (FT)

ORCID ID: orcid.org/0000-0003-4721-1297

[1] Current affiliation: Center for Systems Integration and Sustainability, Michigan State University, East Lansing, MI

Abstract

Forest landscape simulation models (FLSMs) – often used to understand and project forest dynamics over space and time in response to environmental disturbance – have rarely included realistic epidemiological processes of plant disease transmission and impacts. Landscape epidemiological models, by contrast, frequently treat forest ecosystems as static or make simple assumptions regarding ecosystem change following disease. Here we present the Base Epidemiological Disturbance Agent (EDA) extension that allows users of the LANDIS-II FLSM to simulate forest pathogen spread and host mortality within a spatially explicit forest simulation. EDA enables users to investigate forest pathogen spread and impacts over large landscapes (>10^5 ha) and long time periods. We evaluate the model extension using *Phytophthora ramorum* as a case study of an invasive plant pathogen causing emerging infectious disease and considerable tree mortality in California. EDA will advance the utility of LANDIS-II and forest disease modeling in general.

Keywords: LANDIS-II, Forest landscape model, Pathogen, *Phytophthora ramorum*, Disturbance, Epidemiological model

Software name: Base EDA for LANDIS-II

Programming Language: C#

Available at: http://www.landis-ii.org/extensions

Source Code: https://github.com/LANDIS-II-Foundation/Extension-Base-EDA

Reproducible Analysis Repository: https://github.com/f-tonini/LANDIS-II_EDA_CaseStudy

1. Introduction

Epidemiological disturbances, such as emerging pathogens and infectious disease outbreaks, are important agents of forest change around the world, causing tree mortality at scales ranging from individual trees of a single species to entire forest patches (Meentemeyer et al., 2008; Welsh et al., 2009). Beyond the complete loss of certain tree species, forest pathogens can significantly alter the functioning of forested ecosystems and the services they provide (Liebhold et al. 1995, Simberloff 2000, Vitousek et al. 1997). For example, pathogens can reduce the capacity of forests to sequester carbon, and can strongly interact with other types of disturbance such as fire, insects, and drought (Anderson et al. 2004, Dale et al. 2009, Dwyer et al. 2004, Jactel et al. 2012, Vitousek et al. 1997). Developing a better understanding of how forest pathogens interact with other disturbances and changing environmental conditions to alter forest ecosystem dynamics is crucial for land managers, decision makers, and any stakeholder with multiple local interests involved (Cobb and Metz 2017, Rizzo et al. 2005).

Forest landscape simulation models (FLSMs) have been developed to specifically address management and research questions at landscape scales ($>10^5$ ha) by projecting forest dynamics over space and time (Mladenoff 2004, Scheller and Mladenoff 2007). These models typically include details such as tree age, species and biomass, and are widely used to analyze the influence of disturbances over time as they affect large-scale forest ecosystem dynamics (Thompson et al. 2016). One of several FLSMs, LANDIS-II stands out as a process-based forest landscape model that can include variable time steps for different ecological processes (e.g. succession, disturbance, seed dispersal, forest management, carbon dynamics) and simulate their interactions as an emergent property of the independently simulated processed (Mladenoff 2004, 2005, Scheller et al. 2007). LANDIS-II continues to grow its user community and several

extensions are available to simulate disturbances like wind, fire, insects, harvesting, or land-use change. To date, the representation of forest pathogen and disease spread in FLSMs including LANDIS-II has been lacking.

Landscape epidemiological models frequently treat forest composition and host density as static (Meentemeyer et al. 2012), meaning that the species do not age or experience effects of disturbance. This makes it difficult to understand how disease alters competitive interactions among species, a process known as apparent competition, which can alter species composition at a landscape level (Cobb et al. 2010). This lack of realistic changes in host community composition greatly impedes modeling the interactions of other landscape-level disturbances with disease spread (Cobb and Metz 2017).

In this paper, we fill this gap by introducing the Base Epidemiological Disturbance Agent (EDA) extension for LANDIS-II, which simulates forest pathogen spread and mortality in forested landscapes. The new extension is compatible with all LANDIS-II succession extensions and can be used in conjunction with other disturbance extensions (e.g., fire, insect, wind) to simulate their combined effects on forest landscape dynamics. In this paper, we provide an overview of the modeling framework behind Base EDA and an example application of the extension to simulate the expansion of the pathogen (*Phytophthora ramorum*) that causes "sudden oak death" within the Big Sur area of California (USA).

2. Model description

LANDIS-II is a raster-based modeling framework consisting of a model core that links, parses, and validates data from multiple extensions (modules) and allows the user to "plug in" a forest succession extension and any number of optional disturbance extensions (Scheller et. al.

93 2007). EDA is a disturbance extension compatible with all LANDIS-II succession extensions. It
94 is open source and freely available at the LANDIS-II website[2]. The download comes with an
95 installer, user guide and sample data.

96 Base EDA requires the user to supply a raster map with location(s) of initial infection.
97 The user must also supply agent-specific parameters such as host transmissivity, host
98 susceptibility, climate tolerances and preferences, mean transmission rate, acquisition rate,
99 maximum dispersal distance, and choose the appropriate dispersal kernel and exponent (see
100 Sections 2.1-2.3 below). The user also provides parameters defining how other disturbances
101 modify likelihood of infection. We demonstrate Base EDA with a case study of *Phytophthora*
102 *ramorum*, the pathogen which causes sudden oak death, a major forest disease in California
103 (Meentemeyer et al. 2008, 2012, Metz et. al. 2017). For sudden oak death, fire kills the pathogen
104 and slows reinfection for several years following fire (Beh et al. 2012).

105 Base EDA is specifically designed to simulate asymmetric weather-driven transmission
106 of pathogen infection within a multi-host landscape. Transmission is modeled as a dynamic
107 process affecting a meta-population comprised of N contiguous subpopulations represented by
108 cells (sites) arranged on a grid. Cells contain forest tree species age cohorts, and (optionally)
109 nonforest vegetation types. Tree mortality simulated by EDA is passed to the succession model
110 that in turn handles vegetation response to that mortality (e.g., changes in light, water, and/or
111 nutrients, depending on the succession extension used). Epidemiological disturbances within the
112 EDA are probabilistic at the site level, where each site is assigned a probability of being in one
113 of the following states: Susceptible (S), Infected (infectious non-symptomatic) (I), Diseased
114 (infectious and symptomatic) (D). Probabilities are compared with a uniform random number to

[2] www.landis-ii.org

115 determine whether the site becomes infected or, if already infected, to become diseased. Disease
116 causes species- and cohort-specific mortality in the cell. The epidemiological model is similar to
117 that in Meentemeyer et al. (2011) with adjustments made to fit the LANDIS-II framework and
118 account for mortality. Additionally, the model can handle more than one EDA agent (pathogen),
119 and is most compatible with aerial dispersal.
120
121 **2.1 Site Host Index**
122 Site host index (SHI) was adapted from the "site resource dominance" concept in the
123 LANDIS-II Biological Disturbance Agent Extension (Sturtevant et al. 2004). SHI accounts for
124 the spatial distribution of known hosts of the EDA agent and is a combined function of tree
125 species composition and the age cohorts present on that site. This approach allows the
126 quantification of susceptibility for each non-infected cell to become infected, and the suitability
127 of each infected cell to produce infectious spores. The relative host index value of a given
128 species cohort is defined by its host competency class, where low, medium, and high
129 competency classes are user-defined using values ranging between 1 and 10, with non-hosts
130 having a value of 0. The EDA extension compares a look-up table with the species cohort list at
131 each cell generated by LANDIS-II to calculate SHI at time *t* using one of two methods: 1) the
132 host value from the maximum host competency class present, or 2) an average host value of all
133 tree species present, where the host value of each species is represented by the one assigned to
134 the oldest cohort. Species identified as "ignored" do not contribute to the calculation of average
135 resource value, while non-host species that are not ignored contribute a value of 0. Non-
136 sporulating hosts (i.e. hosts that do not contribute to pathogen or disease transmission) should not
137 be included in the host index calculation.

2.1.1 Site host index modifiers

Site host index modifiers (SHIMs) are optional parameters used to adjust SHI to reflect variation introduced by both site environment (i.e., land type) and recent disturbances (Sturtevant et al. 2004). Land type modifiers (LTMs) and disturbance modifiers (DMs) can range between -10 and +10, and are added to the SHI value of all affected sites where host species are present (SHI > 0). LTMs are assumed to be constant for the entire simulation, while DMs have a defined duration and decline linearly with the time since last disturbance (t_{DST}) as follows:

$$DM_{DST}(t) = DM_{max,DST} * \frac{DM_{duration,DST} - t_{DST}}{DM_{duration,DST}}$$

Disturbances that may affect a given EDA agent include fire, wind, other EDA agents and insects, as well as timber harvest. SHI is then modified by LTM and the sum of all DMs:

$$SHIM(t) = SHI(t) + LTM + (DM_{wind}(t) + DM_{fire}(t) + \cdots)$$

The user should calibrate the two modifiers to reflect the relative influence of species composition/age structure, the abiotic environment, and recent disturbance on SHI. SHIM is normalized by its mean over the entire study area, $SHIM(t) = \frac{SHIM(t)}{SHIM_{mean}}$, and modifies the disease transmission rate, β (see Section 2.2). Normalization of SHI allows comparison of β against homogeneous landscape conditions (where SHIM = 1) and to interpret β as the rate of secondary infection of cells by a single infected neighboring cell in an otherwise uninfected landscape.

2.2 Weather

An *annual weather index*, $w(t)$, is used to account for the effect of weather conditions on the probability of uninfected hosts becoming infected, and infected hosts spreading an individual EDA agent. Weather predictors (or transformations thereof) should be selected based on their relevance to the chosen EDA agent. The weather index is multiplied by a baseline transmission rate, β_0, to produce a time-dependent transmission rate, $\beta(t) = w(t)\beta_0$, where β_0 is defined by the user. The basic weather index for year *t*, $W(t)$, comprises the cumulative effect of *N* weather predictors (e.g. rainfall alone, or rainfall and temperature) over a range of months, specified by the user (e.g. April to June), and is calculated as follows:

$$W(t) = \sum_{d \in [month_A(t),\ldots,month_B(t)]} X_1 * X_2 * \ldots * X_N \quad (1)$$

where $X_1 * X_2 * \ldots * X_N$ represent the weather predictors and the cumulative sum runs over days *d* included between two user-defined months ($month_A$ and $month_B$) for the current year *t*. If necessary, weather predictors in (1) can be replaced by derived (e.g., aggregated, or transformed) versions. As an example, a predictor can be aggregated (summed or averaged) over *N* consecutive days of a week or month (e.g., cumulative precipitation). Transformed predictors are expressed by a function, (X). In the current version of the extension (v1.0), only a polynomial transformation is available for the user, defined as:

$$f(X) = A + B + exp(C * \left[\ln\left(\frac{X}{D}\right)/E\right]^F)$$

where A, B, C, D, E, F are constants specified by the user to adjust the shape of the polynomial (e.g., improving polynomial fit to empirical data on response of EDA agent to changes in temperature). As an example, such a transformation can reflect changes in rate of pathogen sporulation at increasing temperature values. The actual weather index, $w(t)$, is normalized by the mean W_{mean} over the available time series of historical weather predictors: $w(t) = W(t)/W_{mean}$. Normalization means that β_0 can be interpreted as the annual transmission rate

under average (or under constant) weather conditions. The weather index built this way varies annually, but is spatially-uniform within each ecoregion.

2.3 Epidemiological Processes

The epidemiological model shares features with spatially-structured metapopulation models and relies on a few important assumptions: First, only the presence/absence of infection in each cell is accounted for. This simplification ignores a transient effect (occurrence, spread and intensification) within the same cell, assuming that an effective level of inoculum is reached rapidly (but still below the maximum sporulating capacity of the cell). Improving this approximation would require a much larger computational effort in the parameter estimation procedure described in Filipe et al. (2012). Second, infected cells immediately become infectious, which is particularly true for an EDA with a small latent period across its host range. Third, infected sites remain infectious for an undetermined (i.e., long) period; in epidemiological terms the infectious period is considered indefinite and is left out of the model. The practical implication is that no cell can recover from infection throughout the simulation, for example by a within-host process such as a host defensive response. However, conversion from infected to uninfected status of a cell can occur due to 1) mortality of susceptible species by disease or other disturbances and/or 2) successional processes that result in a community with no hosts.

At every time step *t*, a susceptible cell (site) *i* can become *cryptically infected* subject to a force of infection $\Lambda_i(t)$ and, once infected, it can become diseased at rate r_D. Despite potentially containing dead hosts, *symptomatically infected* (diseased) cells have the same transmission rate, i.e., are as infectious as cryptically infected cells. The probabilities that cell *i* is in each of the possible states (Susceptible, Infected, Diseased), $P_{i,S}$, $P_{i,I}$, and $P_{i,D}$, respectively, are governed by

a system of differential equations:

$$\frac{\Delta P_{i,S}}{\Delta \mathrm{t}} = -\Lambda_i(t) P_{i,S}$$

$$\frac{\Delta P_{i,I}}{\Delta \mathrm{t}} = \Lambda_i(t) P_{i,S} - r_D P_{i,I}$$

$$\frac{\Delta P_{i,D}}{\Delta \mathrm{t}} = \mathrm{r}_D P_{i,I}$$

The initial conditions for each cell, at the estimated time of onset of the outbreak, are $P_{i,S} = 1$, $P_{i,I} = 0$, $P_{i,D} = 0$, except at the cell estimated to be the location of the first infection, where $P_{i,S} = 0$, $P_{i,I} = 1$, $P_{i,D} = 0$. The force of infection, $\Lambda_i(t)$, is given by:

$$\Lambda_i(t) = \beta(t) \sum_{j \neq i} SHIM_j(t) * SHIM_i(t) * P_{j,I+D|i,S} * K(d_{ij}) \qquad (2)$$

where $\beta(t) = w(t)\beta_0$ is the transmission rate, with $w(t)$ the annual index of weather fluctuation about a *N*-year average (see Section 2.2) and β_0 the baseline rate; $K(d_{ij})$ is a dispersal kernel (see Section 2.3.1) for a given distance *d* between target and source cells; $P_{j,I+D|i,S}$ is the conditional probability that source cell *j* is infectious (either cryptic or symptomatic infection) given that target cell *i* is susceptible. To achieve a first order of approximation, we assume that $P_{j,I+D|i,S} \approx P_{j,I} + P_{j,D}$ which we expect to be a reasonable approximation to the infection pattern, especially when dispersal is not too localized (e.g. within short distance from source of infection).

2.3.1 Dispersal kernel

The dispersal kernel used in Base EDA is derived from, and shares code with, the seed dispersal kernel developed by Lichti and colleagues (N. Lichti, Purdue University, unpublished manuscript). This dispersal function and associated distributions are especially suitable for aerially dispersed EDA agents that include a broad range of fungi and mistletoes. The probability

that the agent disperses a distance *d* from the source was expressed by two main functional forms, often used in the literature: a power-law and a negative exponential. Their generic form can be defined as follows:

$$K_{PowerLaw}(d) = d^{-\alpha}$$

$$K_{NegExp}(d) = e^{-d/\alpha}$$

An EDA agent produced in a source cell can only be deposited in a cell different from the source, i.e., transmission in force of infection (Λ, see Section 2.3 above) is conditional on the agent being dispersed outside the source cell. The rationale for this choice is that infection processes within a cell are not tracked (no transient effect). In addition, the kernel must integrate to 1 within a chosen 2D spatial neighborhood window (excluding the source cell). The 2D window accounts for all possible pathways through which the target cell can become infected by a given source cell. A user-defined maximum radial distance is used to limit EDA agent dispersal within a chosen neighborhood size. For cases where only local, short-distance dispersal events are considered, this parameter becomes essential to reduce computational burden. Only isotropic dispersal (no wind-assisted directional spread) was considered for version 1.0 of the Base EDA extension.

2.3.2 Tree species cohort mortality

Within each diseased cell, the mortality of individual tree species age cohorts is a probabilistic function of the mortality probability of the cohort's vulnerability class. The user defines which species and ages fall into each vulnerability class (low-high), and the probability of cohort mortality for each class. Probabilities are compared with a uniform random number to determine whether an entire age-cohort dies (i.e. is removed) or not, where tree species cohort

250 mortality is then passed to the succession extension which handles the removal of the cohort(s)
251 and updates the cohort list. We acknowledge that complete cohort removal rather than a partial
252 one may be a simplistic assumption in the current version of the model, but for many landscape-
253 level processes or dynamics it should not cause significant changes in outcome. The Base EDA
254 time step concludes updating the time since last disturbance, updating the time since last
255 disturbance, outputting maps of cell states (1 = Susceptible, 2 = Infected, 3 = Diseased) and
256 cohort mortality, and by updating the Base EDA log file (Fig. 1).
257

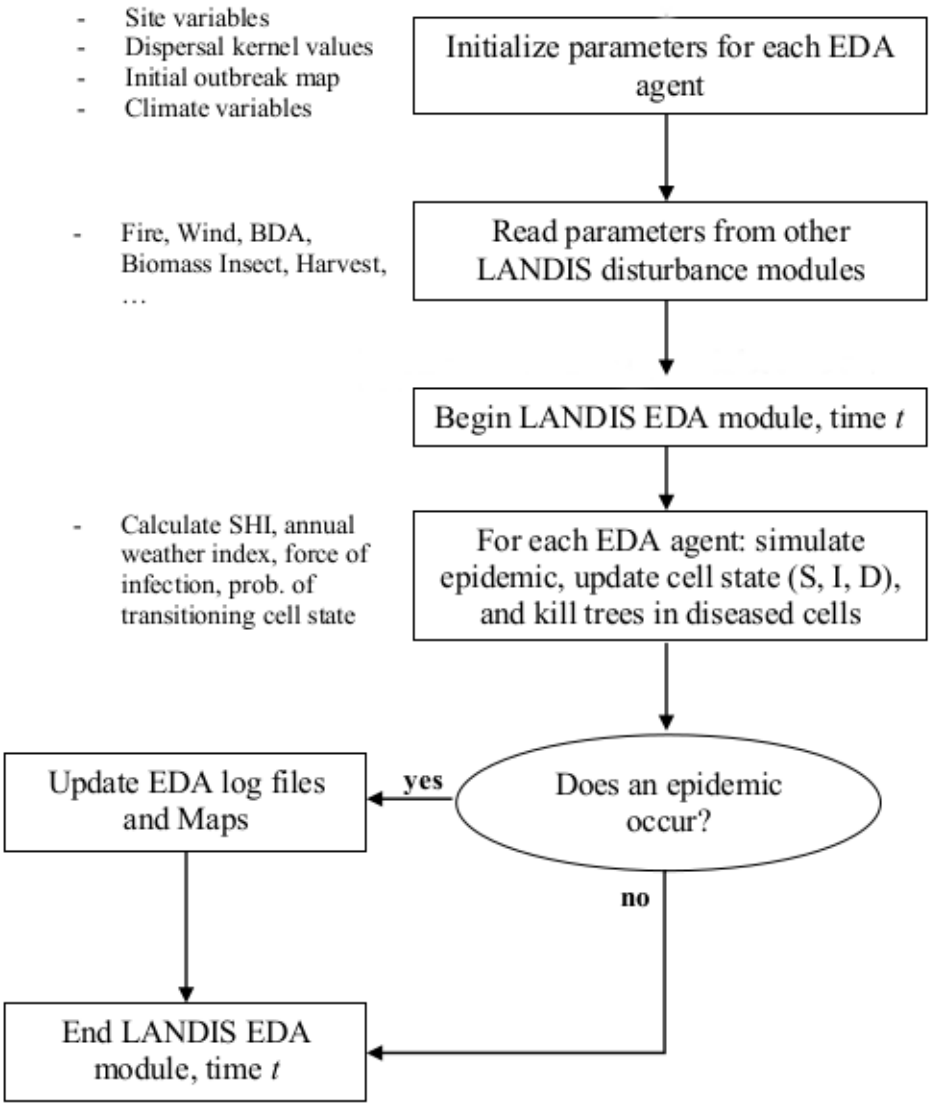

Figure 1: Flow diagram illustrating the main logical structure of the LANDIS-II Base Epidemiological Disturbance Agent (EDA) extension.

3. Case study

To demonstrate the capabilities of the Base EDA extension, we modeled 23 years of *Phytophthora ramorum* spread within an 8,017 km^2 area of central California, USA (Fig. 2). *P. ramorum* infects multiple hosts with some tree and shrub species experiencing non-lethal foliar

symptoms known as ramorum blight, and oaks and tanoaks experiencing lethal stem cankers that lead to the disease sudden oak death. The simulations were initiated with the best-known locations of initial infection in the study area in 1990 and simulated through 2013 (the last year for which plot level infection data are available) (Gaydos et. al. 2017, Metz et. al. 2017). We used LANDIS-II NECN Succession 1.0 (Scheller et al. 2011) to simulate forest growth and succession and the LANDIS-II Base EDA 1.0 extension to simulate spread of *P. ramorum* and mortality caused by SOD. Parameter values chosen for the EDA agent in this simulation are reported in Supplementary material Appendix 1, Table A1-A2. The simulations used a 30-m cell size. Base EDA used 1-year time steps and NECN used 10-year time steps. We compared the simulated disease spread in 2006, 2007, 2009, 2010, 2011, and 2013 with the subset of plots that were sampled in that year (i.e. plots sampled in 2006 were compared to model results in 2006 etc.) (Fig. 2) (Meentemeyer et. al. 2008, Metz et. al. 2017). We achieved a simulation accuracy of approximately 73.05% and 58.33% for infected and uninfected plots, respectively, for an odds ratio of 3.79 (Table 1). Calibration would allow for this to be further improved. Currently, the model is not predicting negative values as well as it does for positive values. Further calibration should improve this behavior. Moreover, it is partially due to the fact that the host data being used for the model are only 80% accurate at the landscape level.

The results also replicate the patchy nature of *P. ramorum* infection observed in the field (Meentemeyer et. al. 2008, Metz et. al. 2017). This example illustrates the utility of being able to simulate disease spread and mortality with an existing FLSM to understand not only the spread of the disease, but also its potential impacts to the ecosystem through mortality of host trees.

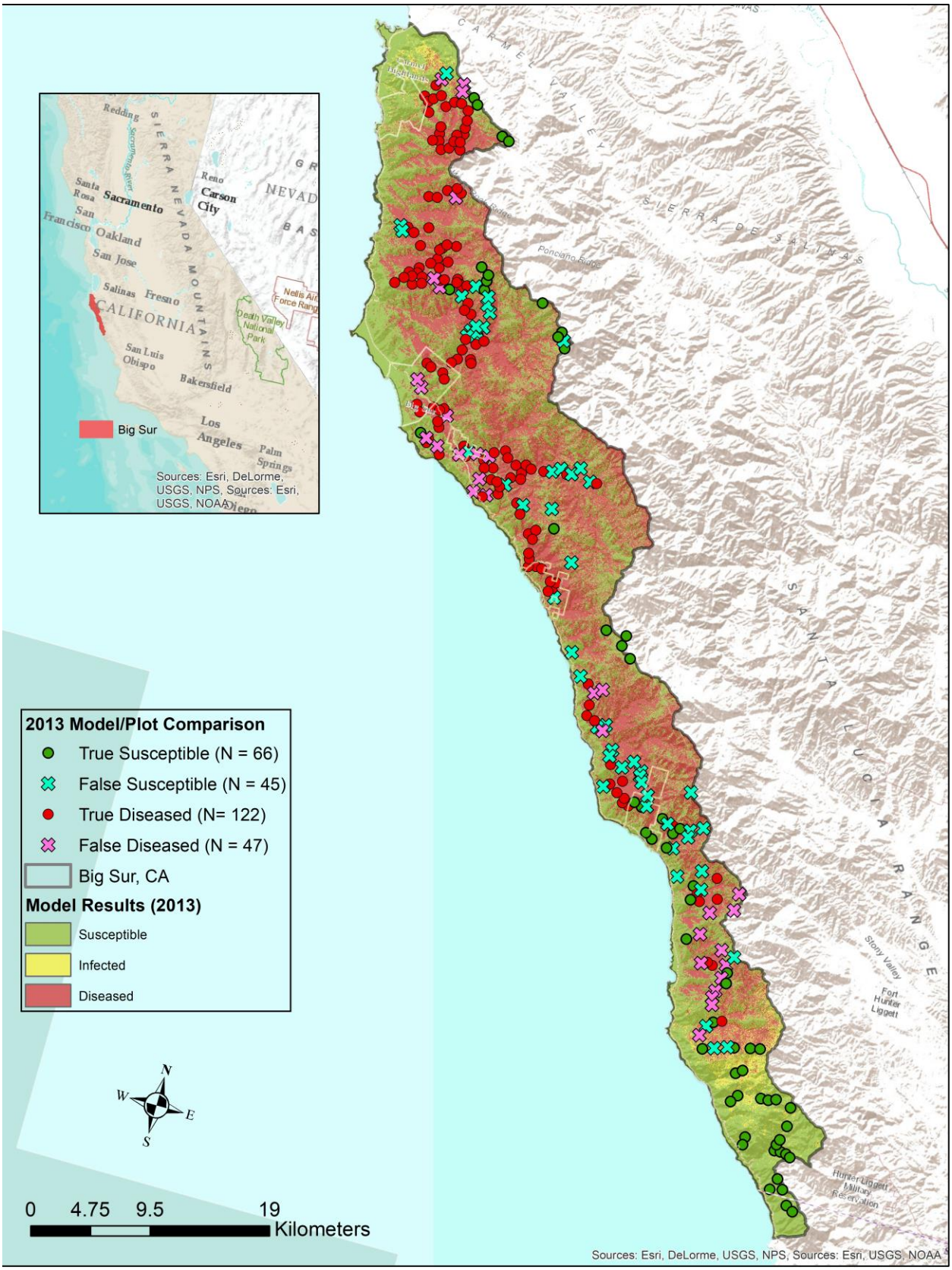
Redding
Santa Rosa
Sacramento
San Francisco
Oakland
San Jose
Salinas
Fresno
CALIFORNIA
San Luis Obispo
Bakersfield
Los Angeles
Palm Springs
Big Sur
Reno
Carson City
Death Valley National Park
Sources: Esri, DeLorme, USGS, NPS, Sources: Esri, USGS, NOAA
CARMEL VALLEY
SIERRA DE SALINAS
Ponciano Ridge
SANTA LUCIA RANGE
Stony Valley
Fort Hunter Liggett
Hunter Liggett Military Reservation
2013 Model/Plot Comparison
True Susceptible (N = 66)
False Susceptible (N = 45)
True Diseased (N= 122)
False Diseased (N = 47)
Big Sur, CA
Model Results (2013)
Susceptible
Infected
Diseased
N
W
E
S
0 4.75 9.5 19
Kilometers
Sources: Esri, DeLorme, USGS, NPS, Sources: Esri, USGS, NOAA

287

Figure 2: 2013 most recent plot disease status compared to 2013 model results. For comparison we used modeled diseased status and most recent plot diseased status (not all plots are sampled every year so this comparison will tend to underestimate plot disease status). For simplicity and realistic comparisons, we treated both infected and uninfected model results as uninfected since infected non-symptomatic areas would be recorded as uninfected in the field due to no visible symptoms.

Table 1: Accuracy assessment of the model results at a landscape level comparing plot observations to model observations for the year the observations occurred (e.g. plots sampled in 2007 were compared to model results in 2007). The true positive rate is 73.1% and the true negative rate is 58.3% and total accuracy is 68.9%. Values are aggregates of all years considered in the model.

		Observed	
		Positive	Negative
Modeled	Positive	225	50
	Negative	83	70
		73.1%	58.3%

We performed a sensitivity analysis of the model's transmission rate (β_0) and the α coefficient in the dispersal kernel. We choose to focus on both β_0 and the α coefficient as they are the parameters that will allow the user most flexibility when calibrating the model and they will have substantial impact on spread. For this analysis we focused on model accuracy as measured by the odds ratio. We ran 3 simulations of each model with a different random seed in order to account for stochasticity between model runs. β_0 varied from 4.00 to 5.00 in 0.25 increments and α varied from 2.4 to 2.6 in 0.1 increments for a total for 15 different combinations of β_0 and α and

total number of model simulations of 45. On average decreasing β_0 by 0.25 resulted in a 7.01% decrease in the odds ratio (a measure of accuracy) while holding α constant. On average a 0.1 decrease in α resulted in a 15.2% increase in the odds ratio while holding β_0 constant.

More broadly, the Base EDA extension could be a suitable landscape modeling tool for a range of EDA agents. Across the globe, an increasing number of destructive pathogens have emerged as disturbance agents shaping forest structure and function at landscape scales. These events have substantial ecological and economic impacts, the understanding of which are important to designing management responses (Liebhold et al. 1995, Simberloff 2000, Vitousek et al. 1997). The default Base EDA data and parameterization is most suitable for aerially dispersed pathogens and those where a biologically-driven infectious period is not a significant factor. These conditions are met for the most destructive forest diseases in North America including chestnut blight, sudden oak death, and possibly Beech Bark Disease although the latter system involves an insect that may complicate the process of infection and spread. In practice, we emphasize the importance of parameterizing the dispersal kernel for application to a new system. Proper understanding of dispersal dynamics is critical to accurate forecasting of spread and disease dynamics (Meentemeyer et al. 2011; Filipe et al. 2012; Metz et al. 2017). Acquiring empirical measurements of dispersal at scales more than a few meters is challenging but we emphasize it is incumbent on users to overcome this difficulty in order to properly apply the model. Examples of confronting this problem for *P. ramorum* can be found in Meentemeyer et al. 2011 and Filipe et al. 2012. These examples integrated several datasets to estimate and validate dispersal parameters including spore trapping, molecular data, landscape-extent monitoring plot networks, and aerial tree mortality mapping from fixed-wing aircraft. We encourage further experimentation with alternative formulations of dispersal kernels and

environmental (weather) dependencies as these could render the extension suitable for a greater range of epidemiological disturbance agents such as pathogens spread via insect vectors, movement of contaminated soil or plant material, and spread in waterways.

Acknowledgments

The authors would like to thank the anonymous reviewers for their valuable comments and suggestions to improve the quality of the paper. The authors thank all members of the Meentemeyer Landscape Dynamics Lab at the Center for Geospatial Analytics, Rob Scheller and Eric Gustafson for their feedback and valuable suggestions on the present work. This research was supported by the National Science Foundation [grant numbers DEB-EF-0622677 and EF-0622770] as part of the joint NSF-NIH Ecology of Infectious Disease program. The authors also gratefully acknowledge financial support from the USDA Forest Service e Pacific Southwest Research Station, the USDA Forest Service e Forest Health Protection, State and Private Forestry, and the Gordon & Betty Moore Foundation. All authors made substantial contributions to this work in the following areas: As first author, F.T. led and coordinated the study presented herein, alongside with code development for the epidemiological model. C.J. and B.M. equally contributed to project development and methods. C.J. helped with extensive editing, structuring, writing, and code development needed to parallelize the EDA extension; B.M. contributed code development with extensive efforts on the weather component of the EDA extension, alongside editing the manuscript. R.C. provided expertise on epidemiological processes and contributed to editing the manuscript; B.S. edited the manuscript and provided expertise on LANDIS-II and other ecological disturbances; and R.M. conceived the project and edited the manuscript. B.S. and B.M. are supported by the National Fire Plan of the US Forest Service. We would like to

thank N. Lichti for the use of his code for the dispersal component of the epidemiological process.

References

Anderson, P. K. et al. 2004. Emerging infectious diseases of plants: pathogen pollution, climate change and agrotechnology drivers. - Trends Ecol. Evol. 19: 535-544. https://doi.org/10.1016/j.tree.2004.07.021.

Beh, M. M. et al. 2012. The key host for an invasive forest pathogen also facilitates the pathogen's survival of wildfire in California forests. - New Phytol. 196: 1145–1154.

Cobb, R. C. et al. 2010. Apparent competition in canopy trees determined by pathogen transmission rather than susceptibility.- Ecol 91: 327e333.

Cobb, R. C. and Metz, M. R. 2017. Tree Diseases as a cause and consequence of interacting forest disturbances. - Forests 8: 147. http://www.mdpi.com/1999-4907/8/5/147.

Dale, V. H. et al. 2009. Climate change and forest disturbances. - BioScience 51: 723–734. https://doi.org/10.1641/0006-3568(2001)051[0723:CCAFD]2.0.CO;2

Dwyer, G. et al. 2004. The combined effects of pathogens and predators on insect outbreaks. - Nature 430: 341-345. doi:10.1038/nature02569.

Filipe, J. A. N. et al. 2012. Landscape epidemiology and control of pathogens with cryptic and long-distance dispersal: sudden oak death in northern Californian forests. - PLoS Comp. Biol. 8: e1002328.

375 Gaydos, D. A. et al. 2017. Resilience of diversity-disease risk interactions following wildfire
376 disturbance. - In: Frankel, S. J. and Harrell, K. M. (ed.), Proceedings of the sudden oak
377 death sixth science symposium. Gen. Tech. Rep. GTR-PSW-255, pp. 7.
378 Jactel, H. et al. 2012. Drought effects on damage by forest insects and pathogens: A meta-
379 analysis. - Glob. Change Biol. 18: 267–276. https://doi.org/10.1111/j.1365-
380 2486.2011.02512.x
381 Lichti, N. I. et al. (in prep). Linking landscapes and demography: accounting for propagule
382 pressure in a forest simulation model.
383 Liebhold, A. M. et al. 1995. Invasion by exotic forest pests: A threat to forest ecosystems. -
384 Forest Sci., Monograph. 30: a0001–z0001(1).
385 Meentemeyer, R. K. et al. 2008. Impact of sudden oak death on tree mortality in the Big Sur
386 ecoregion of California. - Biol. Inv. 10: 1243–1255. https://doi.org/10.1007/s10530-007-
387 9199-5
388 Meentemeyer, R. K. et al. 2011. Epidemiological modeling of invasion in heterogeneous
389 landscapes: spread of sudden oak death in California (1990–2030). - Ecosphere. 2: 1-24.
390 Metz, M. et al. 2017. Lessons from 15 years of monitoring sudden oak death and forest dynamics
391 in California forests. - In: Frankel, S. J. and Harrell, K. M. (ed.), Proceedings of the sudden
392 oak death sixth science symposium, Gen. Tech. Rep. GTR-PSW-255, pp. 2-3
393 Mladenoff, D. J., 2004. LANDIS and forest landscape models. - Ecol. Model., 180: 7–19.
394 https://doi.org/10.1016/j.ecolmodel.2004.03.016
395 Mladenoff, D. J. 2005. The promise of landscape modeling: successes, failures, and evolution. -
396 Issues and Perspectives in Landscape Ecol. 90–100.
397 https://doi.org/10.1017/CBO9780511614415.011

398 Scheller, R. M. and Mladenoff, D. J. 2007. An ecological classification of forest landscape
399 simulation models: tools and strategies for understanding broad-scale forested ecosystems. -
400 Landscape Ecol. 22: 491–505. https://doi.org/10.1007/s10980-006-9048-4
401 Scheller, R. M. et al. 2007. Design, development, and application of LANDIS-II, a spatial
402 landscape simulation model with flexible temporal and spatial resolution. - Ecol. Model.
403 201: 409–419. https://doi.org/10.1016/j.ecolmodel.2006.10.009
404 Scheller, R. M. et al. 2011. The effects of forest harvest intensity in combination with wind
405 disturbance on carbon dynamics in a Lake States mesic landscape. - Ecol. Model. 222: 144-
406 153.
407 Simberloff, D. 2000. Global climate change and introduced species in United States forests. -
408 Sci. Total Environ. 262: 253–261.
409 https://doi.org/https://doi.org/https://doi.org/10.1016/S0048-9697(00)00527-1
410 Sturtevant, B. R. et al. 2004. Modeling biological disturbances in LANDIS: a module description
411 and demonstration using spruce budworm. - Ecol. Model. 180: 153–174.
412 Thompson, J. R. et al. 2016. A LANDIS-II extension for incorporating land use and other
413 disturbances. - Environ. Model. Softw. 75: 202–205.
414 https://doi.org/10.1016/j.envsoft.2015.10.021
415 Vitousek, P. M. et al. 1997. Human alteration of the global nitrogen cycle: Sources and
416 consequences. - Ecol. Appl. 7: 737–750. https://doi.org/https://doi.org/10.1890/1051-
417 0761(1997)007[0737:HAOTGN]2.0.CO;2
418 Welsh, C. et al. 2009. The outbreak history of Dothistroma needle blight: an emerging forest
419 disease in northwestern British Columbia, Canada. - Can. J. Forest Res. 39: 2505–2519.
420 https://doi.org/10.1139/X09-159

421

422